International Journal of GEOMATE, Feb., 2020, Vol.18, Issue 66, pp. 62-67
ISSN: 2186-2982 (P), 2186-2990 (O), Japan, DOI: https://doi.org/10.21660/2020.66.9377
Geotechnique, Construction Materials and Environment

SEDIMENT FLOW CHARACTERISTICS AROUND CYLINDRICAL STRUCTURE REGARDING SEABED EFFECTIVE STRESS RESPONSE

*Anh Quang Tran[1], Kinya Miura[2], Tatsuya Matsuda[2] and Taiki Murakami[1]

[1]Graduate School of Architecture and Civil Engineering, Toyohashi University of Technology, Japan
[2]Department of Architecture and Civil Engineering, Toyohashi University of Technology, Japan

*Corresponding Author, Received: 15 June 2019, Revised: 06 Sept. 2019, Accepted: 15 Jan. 2020

ABSTRACT: Stability of onshore and offshore structures subjected to stormy ocean waves is influenced by the soundness of seabed foundation ground, as well as the intensity of wave pressure acting directly on the structures. The seabed soundness would be affected by the change of the seabed surface elevation caused by erosion and/or deposition of sediment. The fluctuating effective stress in the seabed ground, which is induced by sea wave loading, would cause the reduction in seabed stiffness, and then the sediment flow and related scouring of seabed must be also affected by the effective stress fluctuation. The present study proposes a calculation method for sediment traction flow on seabed around cylindrical structures. The calculation method used comprises with linear wave theory, pore-linear-elasticity theory for seabed medium, and empirical sediment traction flow model regarding seawater flow velocity. Although the intensity of sediment traction flow is mainly a function of seawater flow velocity, the sediment traction flow must be also influenced by the soundness of seabed ground. The sediment flow and associated erosion-deposition around upright cylindrical structures of several types were calculated. The characteristic behavior of sediment flow was clarified.

Keywords: Sediment flow, Erosion-deposition, Cylindrical structure, Reflected-diffracted wave, Effective stress

1. INTRODUCTION

When seabed surface is subjected to water pressure change induced by sea wave loading, the fluctuation of pore water pressure and related effective stress are propagated along depth through seabed ground, where the seabed behaves as multi-phase porous continuum. The fluctuation of effective stress causes the reduction of the seabed stiffness, and then liquefaction or fluidization of seabed material may occur under stormy wave conditions. Some damaged structures which were affected by the destabilization of seabed ground have been reported [1]. On the other hand the destabilization of seabed ground would have effects on the sediment flow, and related scouring.

The present study focuses on the sediment flow that is mobilized by traction force from seawater flow; suspended sediment and sheet flow are out of scope of the present study. Although the sediment traction flow is mainly a function of seawater flow velocity, the sediment traction flow would be also influenced by the soundness of seabed ground even under the same seawater velocity on seabed; the sediment flow in a particular direction would be enhanced by the reduction of effective stress near surface. Miura, Morimasa, Otsuka, Yamazaki and Konami [2] explained the combined effect of seawater velocity and effective stress induced by variation of water pressure on sediment flow, and qualitatively examined the direction of sediment flow average per cycle. Tran, Miura, Matsuda and Yoshino [3] proposed an analytical method regarding the effective stress response of seabed for sediment traction flow, and the method was applied to the seabed subjected to travelling wave and stationary wave near line structures. They clarified the characteristics of erosion-deposition behavior of sediment flow quantitatively; the sediment was deposited near nodes, on the other hand seabed was eroded near loops near line structures. The analytical method is modified and applied to the sediment traction flow behavior around cylindrical structures.

2. ANALYSIS METHOD

The analysis method used consists of three processes: a sea wave analysis, a response analysis of seabed ground to sea wave loading, and an evaluation of sediment flow on seabed.

2.1 Sea Wave Analysis

The behavior of sea wave was analyzed in the framework of linear theory for small amplitude waves.

2.1.1 Incident plane wave

The incident wave travelling along x-axis is expressed by seawater surface elevation η_i and velocity potential ϕ_i; flow velocity vector v_i and water pressure p can be calculated as the derivatives of velocity potential ϕ_i;

$$\eta_i(x,y,t)=\frac{H}{2}e^{i(\lambda x-\omega t)} \quad \because \lambda=\frac{2\pi}{L},\quad \omega=\frac{2\pi}{T} \tag{1a}$$

$$\phi_i(x,y,z,t)=i\frac{gH}{2\omega}\frac{\cosh\lambda(h+z)}{\cosh\lambda h}e^{i(\lambda x-\omega t)} \tag{1b}$$

$$v_i=-\phi_{i,i},\quad p=\rho_w\left(\dot{\phi}_i-gz\right) \tag{2}$$

where H, λ, and ω are wave height, wave number, and angular frequency, respectively. And ρ_w is density of seawater, and g is gravity acceleration.

2.1.2 Travelling and stationary waves

The geometry of upright cylindrical structures is presented in Fig. 1 with an incident plane wave. Two extreme cases were considered for comparison. One is zero-radius (no-structure) case in Fig. 2(b): travelling wave simply appears without reflection or diffraction. The other is infinite radius (line structure) case in Fig. 2(c), where stationary wave appears without diffraction. The travelling wave is expressed by Eq. (1b), and the stationary wave is expressed by the following Eq. (3).

$$\begin{aligned}\phi&=\phi_i+\phi_s\\&=i\frac{gH}{2\omega}\frac{\cosh\lambda(h+z)}{\cosh\lambda h}\left\{e^{i[\lambda(x-R_o)-\omega t]}+e^{i[\lambda(-x+R_o)-\omega t]}\right\}\\&=i\frac{gH}{2\omega}\frac{\cosh\lambda(h+z)}{\cosh\lambda h}\cos\lambda(x-R_o)\cdot e^{-i\omega t}\end{aligned} \tag{3}$$

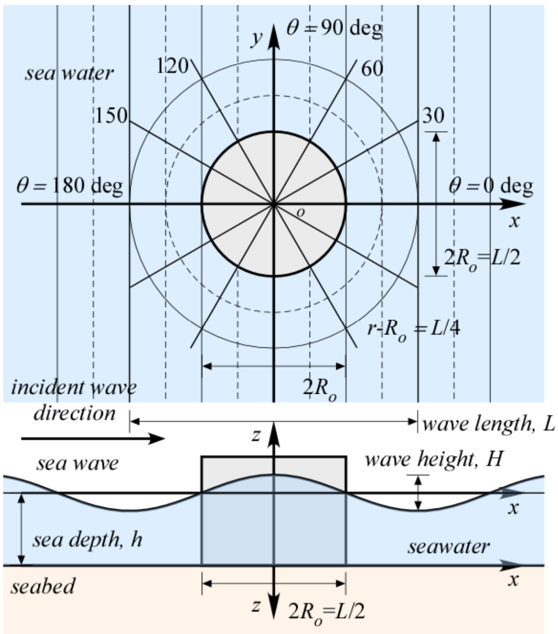

Fig. 1 Upright cylindrical structure

2.1.3 Reflected-diffracted wave for circular cylinder

For the cylindrical structure, the reflected-diffracted wave was generated as a response to the incident plane wave as shown in Fig. 2(a).

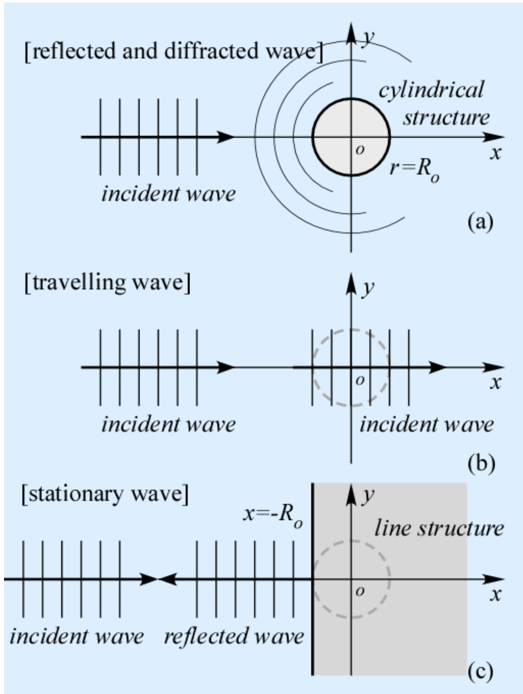

Fig. 2 (a) Reflected-diffracted waves for cylindrical structure, (b) Travelling, (c) Stationary wave for line structure

For the upright cylinder of R_o in radius, MacCamy and Fuchs [4] succeeded in deriving velocity potential according to no-flow condition in radial direction on the side surface as follows

$$v_r=-\partial(\phi_i+\phi_{rdc})/\partial r=0;\quad (r=R_o) \tag{4}$$

$$\phi_{rdc}=-i\frac{gH}{2\omega}\frac{\cosh\lambda\left(h+z\right)}{\cosh\lambda h}\times\left[\sum_{k=-\infty}^{\infty}\frac{J_k{}'\left(\lambda R_0\right)}{H_k^{(1)\prime}\left(\lambda R_0\right)}H_k^{(1)}\left(\lambda r\right)\left(ie^{i\theta}\right)^k\right]e^{-i\omega t} \tag{5}$$

where J_k is Bessel function of first order, and $H_k{}^{(1)}$ is Hankel function of first order.

In the present study, an ocean wave field with uniform depth of 20m was assumed, and an incident plane wave of wave height H of 10m, period T of 13m, wave length L of 167.5m, was employed, regarding the sea wave condition set up for cooperative study by JSCE Committee [5].

2.2 Seabed Response Analysis

The effective stress response of seabed ground to sea wave loading on surface is analyzed with poroelastic continuum model within the framework of linear elastic theory [6]. In the model, seabed material is modeled as a binary phase material consisting with solid phase and fluid phase (mixture of pore water and pore air), and the interaction between the two phases is combined as permeability.

Miura, Asahara, Otsuka and Ueno [7] examined the applicability of the poroelastic continuum model and associated formulations under extensive conditions, according to that the present study employed the u-p formulation under quasi-dynamic, one-dimensional condition in the present study. For a uniform seabed layer with infinite thickness, the fluctuating pore water pressure Δp and associated vertical effective stress $\Delta\sigma_v$ can be calculated as follows.

$$\begin{aligned} &\Delta p(z,t) = \Delta p_o \frac{1}{B_f + E_u}\left(B_f + E_u e^{-\zeta z}\right) e^{-i\omega t} \\ &\sigma_v(z,t) = \Delta p_o \frac{E_u}{B_f + E_u}\left(1 - e^{-\zeta z}\right) e^{-i\omega t} + (\rho_t - \rho_f) z \\ &\quad \because\ \Delta p_o e^{-i\omega t} = \rho_w \dot{\phi},\ z = -h \ \ \text{(on seabed surface)} \\ &\quad \zeta = \sqrt{i\omega h_v} \end{aligned} \tag{6}$$

In the present study, it was assumed that for typical uniform loose sand, uniaxial stiffness of solid phase E_u is $1.40\text{x}10^5$kN/m^2, average stiffness of fluid phase B_f is $0.933\text{x}10^5$kN/m^2, and hydraulic consolidation coefficient H_v is $1.75\text{x}10^{-3}$ s/m^2 (see [5,7] for detailed explanation).

2.3 Evaluation of Sediment Flow on Seabed

The sediment flow and related variation of seabed surface elevation, that is erosion and/or deposition, was calculated in an empirical manner based on the concept of Shields Number, regarding the effective stress response in seabed ground (see Fig. 3).

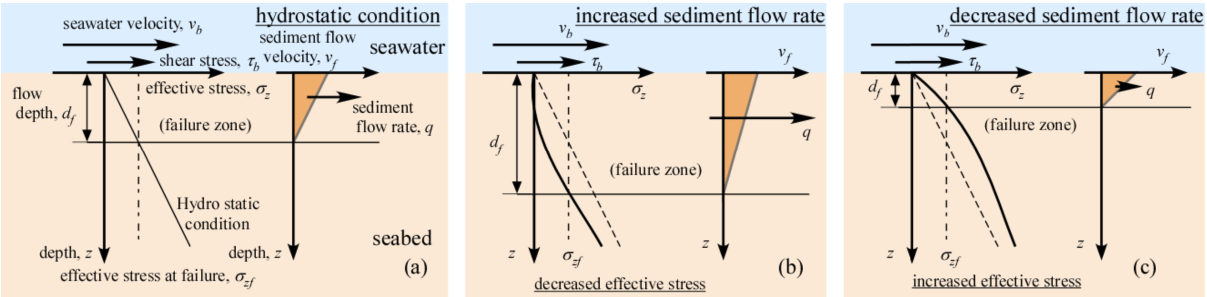

Fig. 3 Sediment flow intensity: (a) hydrostatic pressure condition, (b) decreased effective stress condition, (c) increased effective stress condition

2.3.1 Amount of sediment flow

The surface shear stress τ_b, that is traction force per specific seabed surface area, was assumed to be proportional to the seawater velocity v_b squared as expressed in Eq. (7), where dimensionless coefficient C_b of 1/40 was introduced.

$$\tau_b = C_b \rho_w v_b^2 \tag{7}$$

The sediment would be fluidized within the layer of d_f in thickness, where shear stress τ_b exceeds shear resistance τ_f which is calculated as a function of effective stress σ_z and internal friction angle ϕ_e as shown in Eq. (8). Finally the fluidization depth d_f can be determined.

$$\begin{aligned} &\tau_f = \sigma_z(z,t)\cdot \tan\phi_e, \quad \tau_b = \tau_f \\ &\therefore\ \sigma_z(d_f, t) = \tau_f / \tan\phi_e \end{aligned} \tag{8}$$

Then it was assumed that the distribution of sediment flow velocity v_f within the fluidization layer was triangular along depth as shown in Fig. 3. Thus the amount of sediment flow vector per unit width q (m^2/s) can be calculated with Eq. (9), where the dimensionless coefficient C_q was introduced for the difference between seawater velocity v_b and sediment flow velocity v_f. The value of C_q was assumed to be 1/2.5.

$$q = \frac{1}{2} d_f v_f = \frac{1}{2} d_f C_q v_b \tag{9}$$

As explained schematically in Fig. 3, the amount of sediment flow vector q would be rather dependent on effective stress distribution. Figure 3(a) shows the case of hydrostatic effective stress. If the effective stress decreases, the fluidized shear zone becomes thicker and thus q becomes larger as in Fig. 3(b). On the other hand, if the effective stress increases, the fluidized shear zone becomes thinner and thus q becomes smaller as in Fig. 3(c). It should be noted that even under the same seawater velocity v_b, sediment flow is dependent on effective stress.

2.3.2 Sediment storage rate: erosion-deposition

As shown in Fig. 4, the rate of sediment storage designated as Q (m/s) can be calculated from the total balance of inflow and outflow in both x- and y-directions to/from an infinitesimal rectangular area.

$$Q = -\frac{q_{x(x+\Delta x/2,y)} - q_{x(x-\Delta x/2,y)}}{\Delta x} - \frac{q_{y(x,y+\Delta y/2)} - q_{y(x,y-\Delta y/2)}}{\Delta y} \rightarrow -\left(\frac{\partial q_x}{\partial x} + \frac{\partial q_y}{\partial y}\right) \quad (\Delta x \rightarrow 0, \Delta y \rightarrow 0) \tag{10}$$

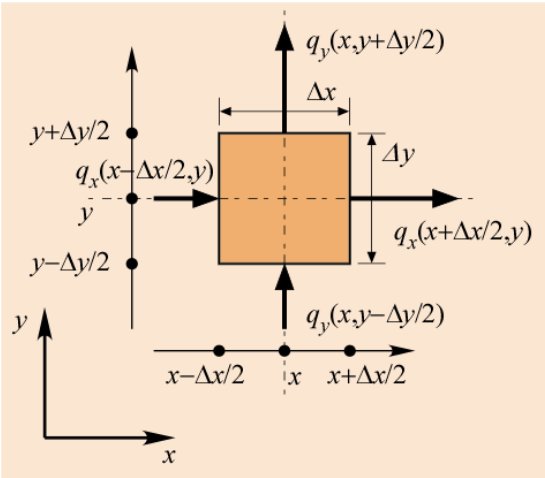

Fig. 4 Calculation of sediment storage from the balance of inflow and outflow to/from infinitesimal rectangular area

The positive and negative values of sediment storage rate Q correspond to deposition and erosion, respectively. The sediment flow velocity vector q and storage rate Q both can be integrated during a sea wave period T for evaluating the accumulated sediment flow behavior; the accumulated integrated values were designated as q_T (m^2) and Q_T (m), respectively.

3. EXAMINATION OF CALCULATED BEHAVIOR AND DISCUSSION

3.1 Sea Wave Behavior around Cylindrical Structure

Figure 5 shows sea wave behaviors along radial directions both in front and back of the cylindrical structure of R_o/L=1/4; the variation of seawater surface elevation along radial direction are drawn in 8 sections of wave period T. For comparative examinations, the travelling wave and the stationary wave are shown in front of the structure (Fig. 5(a): θ =180deg), and the travelling wave is shown in back of the structure (Fig. 5(b): θ =0deg). In the front of cylindrical structure, loop appears on the structure side surface, and node and loop are repeated along the radial direction. Though the loop and node are not clear compared with the stationary wave near line structure, characteristic behavior of stationary wave can be recognized in Fig. 5(a). In back of the structure, sea wave behavior is similar to that of travelling wave with somewhat smaller wave height and a phase lag of about T/4 compared with the travelling wave in Fig. 5(b).

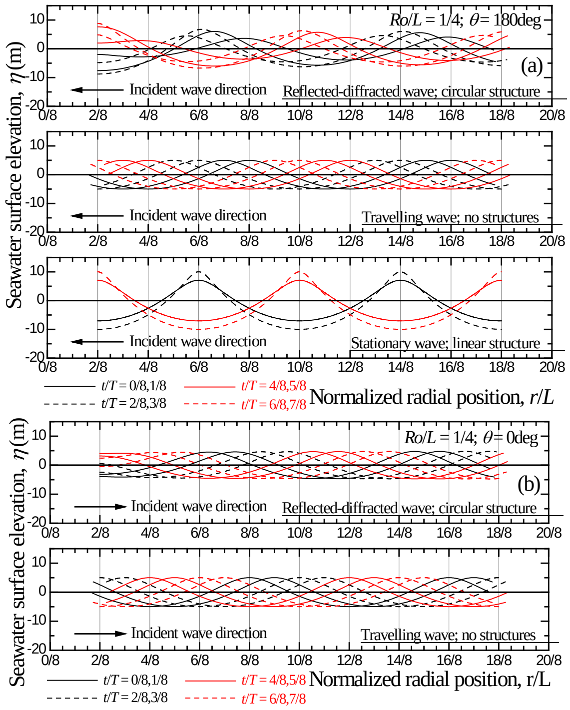

Fig. 5 Behavior of sea surface along radial direction: (a) front of structure, θ =180deg, (b) back of structure, θ =0deg

3.2 Sediment Flow and Storage: Erosion and Deposition around Cylindrical Structure

3.2.1 Behavior in radial direction

Figure 6 shows sediment flow behaviors along radial direction both in front and back of a cylindrical structure of R_o/L=1/4; the variations of accumulated sediment flow vector q_T and sediment storage Q_T are shown in 8 sections of wave period T. For comparative examinations travelling wave and stationary wave are also shown in the figure. In structure front (θ=180deg) radial component of sediment flow vector q_{Tr} is fluctuating but consistently positive. This feature means that the sediment flows away from the structure, and the flow direction is in the opposite of the incident wave travelling direction. The behavior of sediment storage Q_T shows that the seabed is eroded on the side surface, and however, the sediment deposits around the node apart from the structure surface by L/4. The erosion and deposition are seen clearly in the case of stationary wave, and the erosion and deposition are repeated along the radial line in front

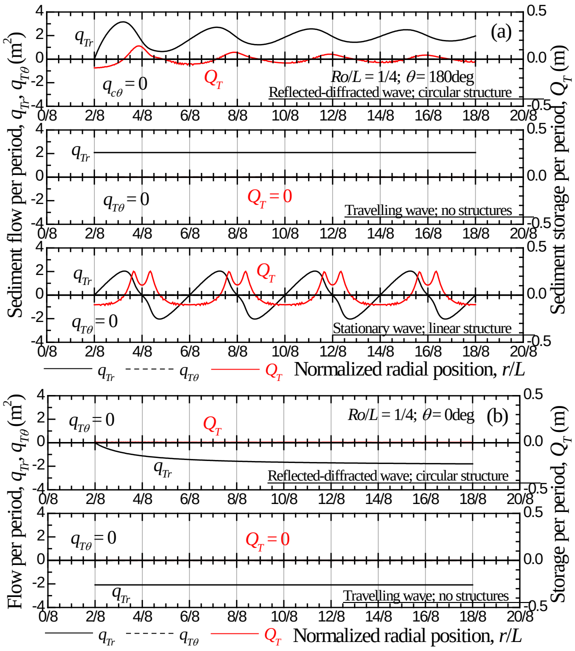

Fig. 6 Behavior of sediment flow on seabed along radial direction: (a) front of structure, θ=180deg, (b) back of structure, θ=0deg

of the structure.

On the other hand, in back of cylindrical structure (θ=0deg), q_T is not fluctuating and consistently negative. This means that the sediment flows toward the structure in the opposite of the incident wave travelling direction. As Q_T is negligibly small, the erosion or deposition wouldn't occur in structure back.

3.2.2 Behavior in circumferential direction

Figure 7(a) shows the behavior of sediment flow and associated storage of sediment on the side wall of the cylindrical structures with different diameters. On the side wall (r=R_o) sediment flows only in circumferential direction. Although the sediment flow is somewhat influenced by the structure size, $q_{T\theta}$ is anti-symmetry and positive on the right hand side but negative on the left hand side in the top of Fig. 7(a). It is suggested that the sediment flows accumulatively from back to front on the structure side surface. The behavior of Q_T tells that notable erosion (Q_T<0) occurs near structure front (θ=180deg), its intensity is equivalent to that in the case of stationary wave.

Figure 7(b) shows the sediment flow behavior on the concentric circle apart from the structure side surface by a quarter of wavelength (r=R_o+L/4). The behavior of $q_{T\theta}$ shows the circumferential flow from structure back to front as similar to the case of on the side surface (r=R_o). The radial flow of sediment q_{Tr} is positive near structure front but negative near the perpendicular directions (θ=+90 or −90deg). On the concentric circle (r=R_o+L/4), notable deposition of sediment (Q_T>0) is recognized around structure front (θ=180deg).

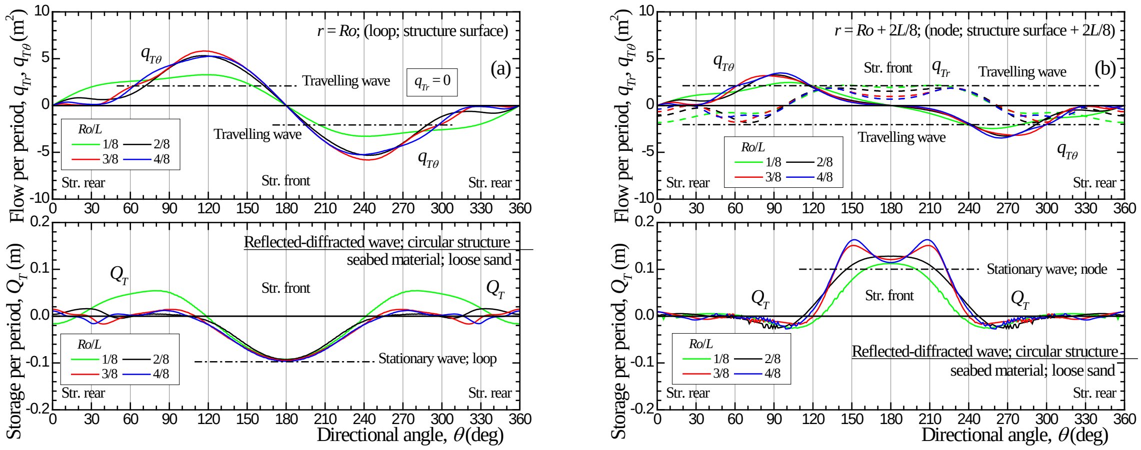

Fig. 7 Behavior of sediment flow along circumferential direction:
(a) (on structure side surface: loop) r=R_o, (b) (on concentric circle: node) r=R_o+2L/8

3.2.3 Plane view of the sediment flow

Figure 8 shows the plane view of sediment flow and associated storage of sediment near the cylindrical structure of R_o = L/4. The red vector indicates the direction and intensity of accumulated sediment flow q_T, and color gradation and contour lines indicate the intensity of sediment storage Q_T. Without structures, the incident wave and travelling wave generate uniform sediment flow with no-storage, in the opposite direction to the incident wave as shown in Figs. 7(a, b) (see [3]). As a result of the disturbances by the cylindrical structure, sediment storage occurs, and erosion and/or

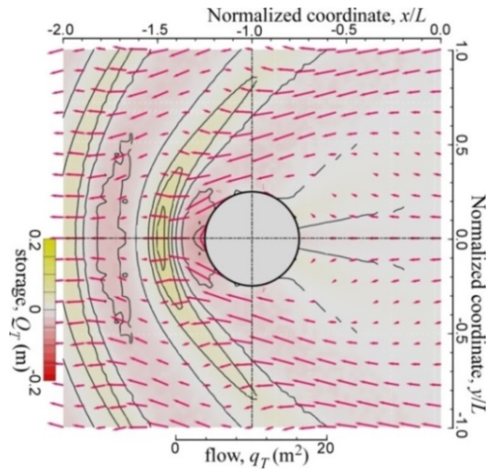

Fig. 8 Plane view of sediment flow and its storage around cylindrical structure: R_o=L/4

deposition are caused.

Figure 9 explains the sediment flow behavior schematically, where arrows are for accumulated sediment flow vector q_T; the thickness of the arrows roughly corresponds to the intensity of q_T. The curved lines indicate the storage of sediment Q_T; the thickness of the lines corresponds to the intensity of Q_T; and light red and light yellow are for erosion (Q_T<0) and deposition (Q_T>0), respectively. Overall behavior of the sediment flow can be explained as follows. Sediment flows toward the structure in the wide range including structure back (–90deg <θ <+90deg). The sediment flows from back to front along structure side surface: the flow is followed by the radial, flows away from the structure in the range including the structure front (120deg<θ<240deg). It should be noted that the erosion and deposition on the parabolic lines are repeated in the wide range of the structure front, which occurs under the influence of sea wave behavior similar to stationary wave with loops and nodes (see Figs. 5, 6). It would be important that the notable erosion on the structure front side surface possibly destabilizes the structure.

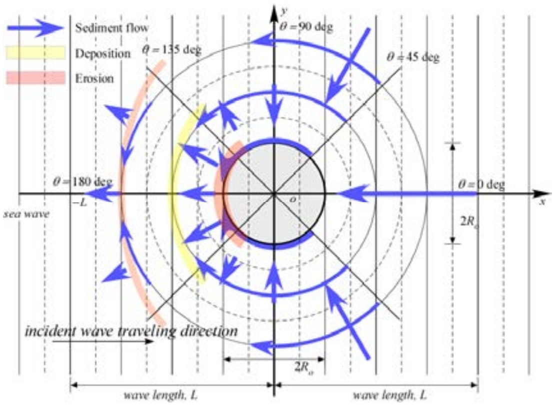

Fig. 9 Schematic explanation of sediment flow behavior around cylindrical structure: R_o=L/4

4. CONCLUSION

The present study explained the analysis method comprised with "the linear wave theory analysis", "effective stress analysis by poroelastic model" and "empirical evaluation method for traction sediment flow", and the sediment flow characteristics when the plane wave meets upright cylindrical structure was examined.

5. ACKNOWLEDGMENTS

The authors are grateful to the Japan Society for the Promotion of Science for its financial support with Grant-in-Aid for Research Activity Start-up 26889035 and Grants-in-Aid for Scientific Research (C)17K06553.

6. REFERENCES

[1] Oka F., Yashima A., Miura K., Ohmaki S. and Kamata A., Settlement of Breakwater on Submarine Soil Due to Wave-induced Liquefaction, 5th ISOPE, Vol.2, 1995, pp.237-242.

[2] Miura K., Morimasa S., Otsuka N., Yamazaki H. and Konami T., Combined Effect of Flow Velocity and Water Change on Wave-induced Seabed Destabilization, J. of Japan Society of Civil Engineers, Ser. B2 (Coastal Engineering), Vol.66, Issue 1, 2010, pp.851-855 (in Japanese).

[3] Tran, A., Q., Miura, K., Matsuda, T., and Yoshino, T., Sediment Flow Characteristics on Seabed Subjected to Stationary Waves with Diagonal Incident Wave Loading Near Line Structures, Proc 8th Int Conf on Geotechnique, Construction Materials and Environment, Kuala Lumpur, Malaysia, 2018, pp.379-384.

[4] MacCamy, R. C. and Fuchs, R. A., Wave forces on piles; a diffraction theory, Tech Memo, No.69, Beach Erosion Board, 1973, pp.1-17.

[5] Coastal Engineering Committee, Coastal Wave, Japan Society of Civil Engineers, 1994, pp.430-503 (in Japanese).

[6] Yamamoto T., H. S. L. Koning and E. Van Hijum, On the Response of a Pore-elastic Bed to Water Waves, J. of Fluid Mechanics, Vol. 87, Part 1, 1978, pp.193-206.

[7] Miura K., Asahara S., Otsuka N. and Ueno K., Formulation of Ground for Coupled Analysis of Seabed Response to Wave Loading, Proc of Symposium on Geotechnical Engineering, Vol. 49, 2004, pp.233-240 (in Japanese).